Article

Modelling and Cost Estimation for Conversion of Green Methanol to Renewable Liquid Transport Fuels via Olefin Oligomerisation

Jenna Ruokonen [1,*], Harri Nieminen [1], Ahmed Rufai Dahiru [2], Arto Laari [1], Tuomas Koiranen [1], Petteri Laaksonen [3], Ari Vuokila [2] and Mika Huuhtanen [2]

[1] LUT School of Engineering Science, Lappeenranta-Lahti University of Technology, P.O. Box 20, FI-53851 Lappeenranta, Finland; harri.nieminen@lut.fi (H.N.); arto.laari@lut.fi (A.L.); tuomas.koiranen@lut.fi (T.K.)
[2] Environmental and Chemical Engineering, University of Oulu, P.O. Box 4300, FI-90014 Oulu, Finland; rufai.dahiru@oulu.fi (A.R.D.); ari.vuokila@oulu.fi (A.V.); mika.huuhtanen@oulu.fi (M.H.)
[3] LUT School of Energy Systems, Lappeenranta-Lahti University of Technology, P.O. Box 20, FI-53851 Lappeenranta, Finland; petteri.laaksonen@lut.fi
[*] Correspondence: jenna.ruokonen@lut.fi; Tel.: +358-40-648-2478

Abstract: The ambitious CO_2 emission reduction targets for the transport sector set in the Paris Climate Agreement require low-carbon energy solutions that can be commissioned rapidly. The production of gasoline, kerosene, and diesel from renewable methanol using methanol-to-olefins (MTO) and Mobil's Olefins to Gasoline and Distillate (MOGD) syntheses was investigated in this study via process simulation and economic analysis. The current work presents a process simulation model comprising liquid fuel production and heat integration. According to the economic analysis, the total cost of production was found to be 3409 €/t$_{fuels}$ (273 €/MWh$_{LHV}$), corresponding to a renewable methanol price of 963 €/t (174 €/MWh$_{LHV}$). The calculated fuel price is considerably higher than the current cost of fossil fuels and biofuel blending components. The price of renewable methanol, which is largely dictated by the cost of electrolytic hydrogen and renewable electricity, was found to be the most significant factor affecting the profitability of the MTO-MOGD plant. To reduce the price of renewable fuels and make them economically viable, it is recommended that the EU's sustainable transport policies are enacted to allow flexible and practical solutions to reduce transport-related emissions within the member states.

Keywords: methanol; MTO-MOGD; hydrocarbon fuels; renewable energy; sustainable transport; process simulation; techno-economic analysis

1. Introduction

The legal framework set by the Paris Climate Agreement [1] calls for practical technological solutions to realise emission reduction targets at both the European Union (EU) and the national levels. The ultimate target of the EU is to gradually achieve carbon neutrality by 2050 [2]. The realisation of considerable emission reductions requires marked reconfiguration of the energy sector. The role of hydrogen in the energy transition has gained significant interest, and the question of whether to use renewable electricity directly as a source of power or to convert electricity to hydrogen via the electrolysis of water remains unresolved. The direct use of electricity in battery electric vehicles is the most energy efficient option, and this can be readily observed by comparing the overall well-to-wheels efficiencies of fully electric vehicles and internal combustion engine vehicles. After taking fuel production, distribution, retail, and vehicle losses into account, the well-to-wheels efficiency of fossil fuel-powered internal combustion engine vehicles is only 25–29%, while the corresponding figure for battery electric vehicles charged with renewable electricity is

68% [3]. However, wide-spread adoption of electric transport is hindered by the scarcity of materials required for the production of batteries. Weil et al. estimated that global lithium and cobalt reserves will be exhausted by 2050, even with high recycling rates for the used battery materials [4]. Additionally, there were 280 million road vehicles in use in the EU in 2019 [5], and 96% of these vehicles operated on either gasoline or diesel and were in use for 12 years on average. Transitioning the entire internal combustion engine vehicle fleet to battery-powered electric vehicles is therefore a slow and demanding process.

The announced auction prices for onshore wind power and solar photovoltaics fell by 49% and 83%, respectively, between 2013 and 2020 [6]. Despite the favourable reduction of renewable electricity prices, the conversion of aviation, long-haul marine transport, and heavy road transport to fully electric alternatives in the near future is challenging. Alternative liquid fuels, such as renewable methanol and ammonia, have been considered as substitutes for fossil fuels in marine transport [7], while jet fuel does not yet have such a sustainable alternative.

The direct use of hydrogen for transportation also has challenges. Large-scale deployment of hydrogen production is restricted by issues related to demanding storage conditions, safety concerns, and insufficient infrastructure [8], and these difficulties further translate to high costs. The use of hydrogen-powered fuel cells is also limited by the low overall technology readiness level (TRL) [9]. It would therefore be preferable to convert renewable hydrogen and carbon dioxide to methanol or liquid hydrocarbons via power-to-liquid (PTL) processes. PTL has gained increasing attention as an alternative route for transport fuel production, especially in hard-to-abate sectors [10]. The International Air Transport Association views the electrification of commercial aviation as unlikely until 2040 [11]; hence, producing liquid aviation kerosene is the most viable option for decades to come. Some major airlines [12,13] have already announced initiatives to begin using carbon-neutral kerosene. Global consumption of aviation kerosene was nearly 300 Mt in 2019, and consumption has increased steadily over the past 15 years with an average annual growth rate of 2.5% [14]. This represents remarkable business potential for PTL processes if fossil kerosene is gradually replaced with synthetic aviation fuel.

There are several methods to convert hydrogen and carbon dioxide into hydrocarbons. In conventional synthetic fuel production, the raw material is syngas, a mixture of CO and H_2, which can be used to synthesise methanol or hydrocarbons. Processes converting CO_2 to hydrocarbons can be divided into direct and indirect methods. Direct conversion technologies constitute Fischer–Tropsch (FT) processes in which syngas is converted to hydrocarbon chains with high carbon numbers [15]. As the FT synthesis uses CO, a reverse water–gas shift reaction must be carried out if CO_2 is utilised as the carbon source [16]. The oil and petrochemical company Shell uses FT synthesis in its Shell Middle Distillate Synthesis (SMDS) plants in Qatar and Malaysia. The process produces synthetic crude that can be refined into liquid fuels [17]. The FT process is also used in South Africa by The Petroleum Oil and Gas Corporation of South Africa (PetroSA) [18]. The plant produces gasoline and diesel fuels via a conversion of olefins to distillate (COD) process by converting light FT olefins to higher olefins. To the best of our knowledge, PetroSA is the only company that uses the COD process [19].

In an alternate conversion process, hydrocarbons are produced via methanol. First, CO or CO_2 is hydrogenated to methanol. The methyl alcohol is then further dehydrated to dimethyl ether (DME) and finally to hydrocarbons. As a result of the series of dehydration reactions, a large quantity of water is formed as a by-product. The first application of methanol for fuel production was ExxonMobil's methanol-to-gasoline (MTG) process [20]. Haldor Topsøe developed the synthesis further and integrated methanol and gasoline production into a single synthesis loop in a process called Topsøe integrated gasoline synthesis (TIGAS) [21]. Both techniques are currently commercially available with a TRL of 9. While these processes produce only gasoline as the main hydrocarbon product, ExxonMobil further developed the methanol-to-olefins (MTO) process and Mobil's olefins to gasoline and distillate (MOGD) process. When these processes are coupled, methanol

can be converted into gasoline, kerosene, and diesel [22]. Because the MOGD process was only developed to the pre-commercial stage in the 1990s [23], the TRL of MTO-MOGD can be estimated to be 8.

Synthesis techniques originally developed for fossil raw materials can be adopted in renewable transport fuel production. CO_2 can be acquired from industrial emissions, biogenic sources, or directly from the atmosphere. Hydrogen can be produced via electrolysis of water using renewable electricity. Methanol production is a well-known and industrially proven technology with fossil raw material sources that mainly uses steam reforming of methane to produce syngas. Renewable methanol is already produced in Iceland from captured CO_2 and renewable H_2 [24]. Further refining of methanol into liquid hydrocarbon fuels is possible in an MTO process where methanol is converted to light olefins and water via a dimethyl ether intermediate. The synthesis is coupled with a MOGD process that converts light olefins into gasoline, kerosene, and diesel range liquid fuels via olefin oligomerisation. The principle of methanol conversion into transport fuels by combining the two processes is illustrated in Figure 1 as a block diagram.
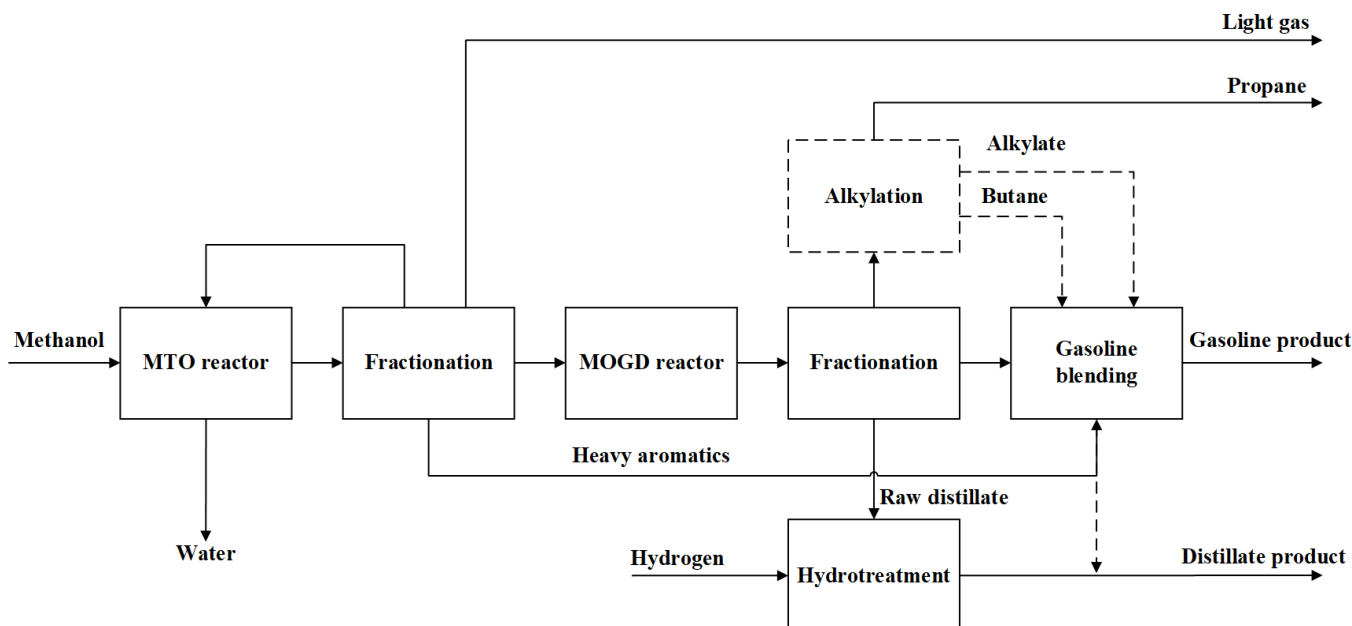
Figure 1. Block diagram of the methanol-to-olefins (MTO) and Mobil's olefins to gasoline and distillate (MOGD) processes. Adapted from Grimmer et al. [25].

The reaction system in the synthesis catalysed by the ZSM-5 zeolite molecular sieve can be described in a generic form via Equations (1)–(3) [26,27]. Equations (1) and (2) describe the hydrocarbon pool mechanism proposed by Dahl and Kolboe [28]. First, methanol (MeOH) is dehydrated to dimethyl ether and water (Equation (1)). Further conversion of DME (Equation (2)) yields additional water and light olefins with a general expression of $(CH_2)_n$, where $2 \leq n \leq 4$ [28]. C_3–C_6 olefins are the main reaction products in Equation (2), but light paraffins, naphtenes, and aromatics with carbon numbers ≤ 10 also form [23]. In the final step (Equation (3)), light olefins are oligomerised to produce higher olefins in the C_5–C_{20} range. Estimates of the standard reaction enthalpies and the corresponding reference values found in literature [29,30] are given in the Supplementary Materials.

$$2n\ CH_3OH \xrightarrow{ZSM-5} n\ CH_3OCH_3 + n\ H_2O. \tag{1}$$

$$n\ CH_3OCH_3 \xrightarrow{ZSM-5} 2(CH_2)_n + n\ H_2O. \tag{2}$$

$$2(CH_2)_n \xrightarrow{ZSM-5} C_{2n}H_{4n} \tag{3}$$
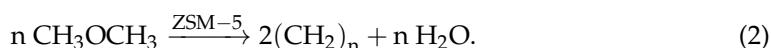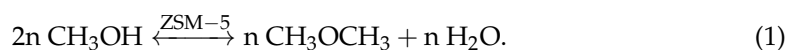
The MTO-MOGD process is often introduced in the literature in connection to synthetic fuel production [31,32]; however, to the best of our knowledge, the process has not been modelled in detail. Baliban et al. [33] presented a synthesis and optimisation scheme for the thermochemical conversion of coal, biomass, and natural gas to liquid hydrocarbons via MTO-MOGD. Baliban et al. [34] also carried out a comparative study of FT and MTO-MOGD for biomass-based processes. Onel et al. [35] introduced a synthesis and optimisation framework focusing on light olefin production from biomass and natural gas. However, these studies considered hydrocarbon formation and refining only via atom balance calculations. As an improvement to the previous studies, the current work introduces a detailed process modelling and economic analysis for the synthesis of gasoline, kerosene, and diesel from renewable methanol. A steady-state process simulation model is created using the Aspen Plus V11 simulation software, and cost evaluation for the process is developed based on the model. A process model integrating the simultaneous production of several liquid fuels, a hydrogen recycling loop, and heat recovery system from fuel gas is a unique approach for further development of the MTO-MOGD process. Additionally, a sensitivity analysis to determine the parameters that most influence the profitability of this process is of great interest to decision-makers.

2. Materials and Methods

The simulation flowsheet was constructed, and the process conditions were determined based on literature references [22,23]. Because the MTO-MOGD process has not reached the commercial scale [23] and reported process information is limited, the design was complemented with approximations using common process engineering principles. For instance, process conditions in the separation stages were defined iteratively to achieve the desired performance. Heat integration within the model was also designed to reduce the energy consumption of the process. The Peng–Robinson (PENG-ROB) method was chosen for physical property estimation as it is applicable for nonpolar and mildly polar mixtures of hydrocarbons and MeOH/DME/water [36]. PENG-ROB was recently found to also be applicable in methanol/hydrocarbon processing by Shi et al. [37] and Henning and Haase [38]. This selection was validated by comparison of the modelling results to those predicted via alternative physical property methods. The process was designed for 3000 kg/h methanol feed, which corresponds to a pilot-scale production plant.

2.1. Process Description

A simulation flowsheet and process flow diagram are shown in Figures 2 and 3, respectively. Further simulation specifications are given in the Supplementary Materials.
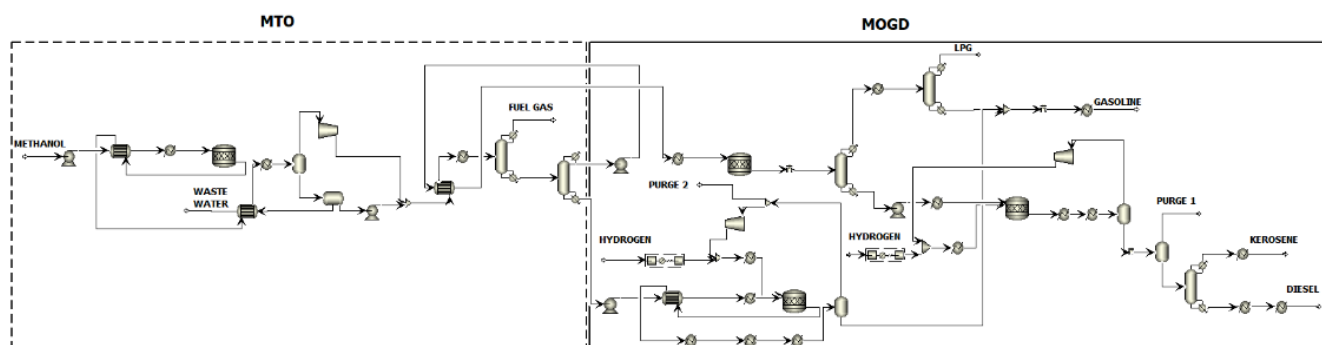
Figure 2. Aspen Plus simulation diagram of the MTO-MOGD model. The MTO section of the process is indicated with a dashed line and the MOGD with a solid line.
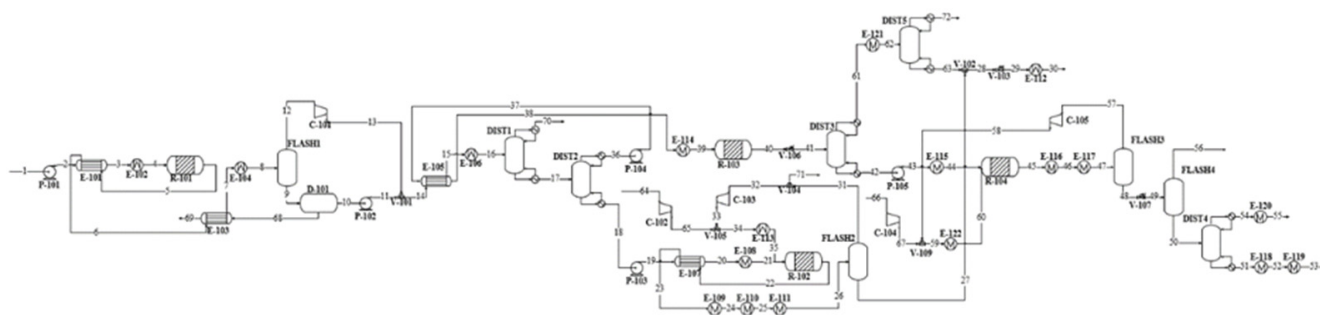
Figure 3. Flow diagram of the MTO-MOGD model.

Methanol is assumed to enter the process under atmospheric conditions. It is pumped and heated to the MTO reactor conditions of 2 bar and 450 °C. In the reactor, methanol is first converted to DME and water, and further to light olefins and additional water. The reactor operates isothermally via high-pressure (HP) steam generation. The reactor effluent is cooled down and water is separated from the hydrocarbon–water system. Non-condensable light hydrocarbon gases are separated from light olefins via distillation and directed to high-temperature heat generation. Durene is separated from the olefin product in the following distillation column and sent to a dedicated heavy gasoline treatment.

The MOGD reactor converts light olefins into heavier olefins via oligomerisation reactions. The reactor operates at 40 bar and 200 °C, and the temperature is kept constant by low-pressure (LP) steam generation. The reactor product is fractioned to liquefied petroleum gas (LPG), gasoline, and distillate products via two-step distillation. The distillate blend formed by olefinic kerosene and diesel compounds is hydrotreated to saturate the carbon–carbon double bonds. The hydrogenation reactor operates isothermally at 40 bar and 300 °C. Exothermic reaction heat is directed to HP steam generation. The paraffinic distillate product is separated from excess hydrogen gas and distilled to separate kerosene and diesel fuels. Hydrogen is recovered at a purity of 99.6 mol% and recycled back to the reactor feed.

The aromatic gasoline fraction rich in durene is treated via hydroisomerisation in a heavy gasoline treatment unit. The isomerisation reaction takes place in the presence of hydrogen gas in an isothermal reactor operating at 16 bar and 345 °C. The reaction heat is provided by high-temperature heat. The durene content of the aromatic fraction is reduced by 57 mol% during the reaction. The resulting hydrocarbon–hydrogen mixture is separated, and the aromatics are blended with the gasoline fraction. Then, 99.7 mol% of hydrogen is recovered at a purity of 99.4 mol% in the separation stage and recycled back to the reactor feed.

Heat is recovered from combustion of light gases removed from the light olefins. The combustion air is pre-heated using HP steam prior to entering the furnace. Overall, 1.1 MW of high-temperature heat >500 °C is recovered from the furnace and cooling of the combustion gases. An additional 0.1 MW is recovered from the combustion gases by generation of high-pressure steam in a flue gas boiler.

2.2. Model Specification

To simplify the complex reaction system of various hydrocarbon compounds, the gasoline was considered as a mixture of C_4–C_{10} paraffins, olefins, naphthenes, and aromatics. The kerosene was estimated to consist only of C_{12} paraffins and olefins, and diesel was assumed to include C_{16}, C_{18}, and C_{20} hydrocarbons. The Supplementary Materials contain the specifications of the model components and the reactions taking place in each reactor.

Operation of the MTO and MOGD reactors R-101 and R-103, respectively, was determined based on the reported operation experience of Mobil's demonstration-scale MTO-MOGD plant [22]. In the model, full conversion of methanol to DME and further conversion to light olefins occurs in reactor R-101. Because of the highly exothermic re-

action system, the reactor was assumed to be equipped with a cooling jacket. In reactor R-103, C_2–C_6 olefins are oligomerised to long-chained olefins with carbon numbers up to C_{20}. The reactions are catalysed using the ZSM-5 catalyst. The yields in both reactors were set to correspond with the experimental yields reported by Avidan [22] by adjusting the fractional conversion of each reaction.

Hydrotreatment of the distillate fraction was modelled based on previously reported work [39]. The hydrogen feed was estimated to be equimolar to the hydrocarbon flow, as suggested by Gong [40]. The hydrogenation reactions were assumed to produce both linear and branched paraffins over a Ni/γ-Al_2O_3 catalyst [41].

The aromatic compound durene (1,2,4,5-tetramethylbenzene) has a melting point of 79 °C, while its two isomers, isodurene (1,2,3,5-tetramethylbenzene) and prehnitene (1,2,3,4-tetramethylbenzene), melt at −24 and −7 °C, respectively [42–44]. High durene content in gasoline can lead to engine issues, especially in cold climates. This can be avoided via treatment of durene by hydroisomerisation. The process was modelled based on the process patented by Topsøe [45]. Isomerisation of durene to isodurene and prehnitene occurs over a sulphided Ni/ZSM-$5/Al_2O_3$ catalyst in the presence of hydrogen gas. Along with the hydrogenation–dehydrogenation activity of the catalyst, cracking and hydrogenolysis reactions occur on a minor scale. It was discovered by Hidalgo-Vivas and Joensen [45] that ~6 vol% of the hydrogen fed to the isomerisation reactor was consumed in the synthesis, while the yield of the C_3–C_7 fraction increased. Thus, it was approximated that n-pentane was formed in this work via the reaction of durene and hydrogen in an amount that corresponds to the reported hydrogen consumption. Hidalgo-Vivas and Joensen did not, however, report the individual quantities of isodurene and prehnitene formed during the hydroisomerisation process. It was therefore assumed that the isomers formed in equimolar ratios. Based on these considerations, the reaction stoichiometry can be presented by Figures 4 and 5.
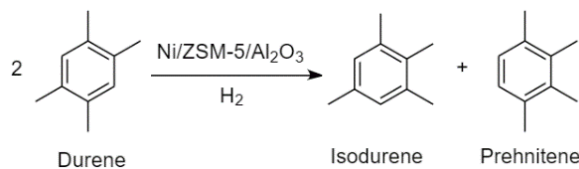
Figure 4. Hydroisomerisation of durene to isodurene and prehnitene over a Ni/ZSM-$5/Al_2O_3$ catalyst.
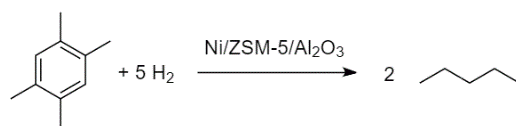
Figure 5. Hydrogenation of durene to n-pentane over a Ni/ZSM-$5/Al_2O_3$ catalyst.

The combustion of light gases in a furnace was modelled using an RGibbs reactor block with an isothermal specification at 1000 °C. Air input was specified at a molar excess of 20% above complete combustion, with combustion air pre-heated to 235 °C using high-pressure steam. The amount of high-temperature heat was calculated via addition of the furnace heat duty and the additional duty from cooling of the combustion gases to 500 °C. The amount of heat recovered as HP steam was calculated as the heat duty from further cooling of the gases to 260 °C.

2.3. Thermodynamic Model Comparison

Performance of a simulation model is conventionally evaluated by validating the model with an external dataset. As the MTO-MOGD process has not been developed into fully commercial scale, extensive experimental data are not available in the literature. The model validity can be alternatively evaluated by critically examining the model setup. The selection of an appropriate Aspen Plus property model is one of the most important steps

and affects simulation of the hydrocarbons. While the Peng–Robinson equation of state is commonly used as a property method for the simulation of hydrocarbons especially in petrochemical processes [36], it was compared to other potential property models for hydrocarbon simulation to justify the selection. The methods selected for comparison include the Peng–Robinson with Boston–Mathias modification (PR-BM), Redlich–Kwong–Soave with modified Huron–Vidal mixing rules (RKSMHV2), and the Soave–Redlich–Kwong (SRK) method. Both the Boston–Mathias modification and the modified Huron–Vidal mixing rules aim to improve the accuracy of these equations of state under high-pressure conditions, and the latter is used in particular when both polar and non-polar components are present [36].

To compare the predictions of each property method, the mass flow rates of the key product fractions were compared to the results given by the PENG-ROB method. The comparisons were made in terms of the relative difference in mass flow rate compared with the corresponding PENG-ROB results, as described by Equation (4):

$$\frac{\dot{m}_{i,n} - \dot{m}_{i,PENG-ROB}}{\dot{m}_{i,PENG-ROB}} \times 100\%. \tag{4}$$

where i refers to the product fraction and n refers to the property method used.

2.4. Economic Evaluation

2.4.1. Capital Expenditure

The fixed capital investment for the MTO-MOGD plant was evaluated using the model in Aspen Plus. The purchased equipment costs ($C_{e,i,CS}$) were calculated using the Aspen Process Economic Analyzer (APEA) tool that sizes the equipment and estimates the costs based on the equipment dimensions. Reactor sizes were manually determined based on the liquid and weight hourly space velocities reported in the literature [40,45,46] rather than using the dimensions calculated by APEA. The purchase costs of the reactors were considered twice to enable a dual reactor configuration in which one reactor is on stream and the other is under catalyst regeneration. Reflux pumps for each distillation column were supplied twice for both the condenser and reboiler cycles.

APEA V11 calculates the equipment costs in the United States on the basis of 2018 Q1. The costs were updated using correction factors for inflation, currency rates, and location [47]. The inside battery limits (ISBL) investment was then calculated using Equation (5) taking equipment installation and commissioning into account. The material factor was considered for equipment manufactured using type SS304 stainless steel instead of carbon steel (CS). For such equipment, SS304 was chosen over CS because of its superior heat and pressure resistance as well as its relatively higher resistance to hydrogen embrittlement. The values of the factors in Equation (5) are listed in Table 1. The total fixed capital cost (TFCC) was calculated using Equation (6) by estimating the shares of outside battery limit (OSBL) costs (OS), design and engineering (DE) charges, and the investment contingency (X) [48].

$$C_{ISBL} = \sum_{i=1} C_{e,i,CS} \left[\left(1 + f_p \right) f_m + f_{er} + f_{el} + f_{ic} + f_c + f_s + f_l \right] \tag{5}$$

$$C_{TFCC} = C_{ISBL} (1 + OS)(1 + DE + X) \tag{6}$$

The MTO-MOGD plant was considered as an independent greenfield site with proprietary auxiliary systems. Towler and Sinnott [48] recommended the use of 40% of ISBL as an initial estimate for the OSBL cost. The share of the OSBL cost can be reduced by using auxiliary infrastructure serving several synthesis plants. The design and engineering as well as contingency charges were also estimated based on values given by Towler and Sinnott [48].

Table 1. Factors used to convert purchased equipment cost to ISBL cost. Factor values adapted from Towler and Sinnot [48].

Factor	Symbol	Value
Material (CS/SS304)	f_m	1/1.3
Piping	f_p	0.8
Equipment erection	f_{er}	0.3
Instrumentation and control	f_{ic}	0.3
Electrical	f_{el}	0.2
Civil work	f_c	0.3
Structures and buildings	f_s	0.2
Lagging and paint	f_l	0.1

2.4.2. Cost of Production

The variable cost of production (VCOP), including the product and by-product revenues; costs associated with the raw materials, consumables, and utilities; and expenditure related to waste management, was calculated. The value for each cost factor is listed in Table 2. Catalyst replacement was assumed to take place every two years, as suggested in the literature [49]. A typical catalyst lifetime in hydrocarbon processing can be expected to vary between 1.5 and 3 years [50,51]. Assumptions for the fixed cost of production (FCOP) and profitability calculations are shown in Table 3. The fixed production costs were estimated as outlined by Towler and Sinnott [52]. The working capital of the plant can be estimated as a share of TFCC or based on the production rate. Towler and Sinnott [53] recommend estimating working capital in the range of 5–30% of TFCC depending on the complexity of raw material inventory and final product storage. In this case, 5% working capital was chosen for the calculations. The investment in the form of working capital is recovered at the end of plant lifetime by liquidating inventories [53]. The interest rate of the loan was estimated to be 2%, which corresponds to the rate of recent large corporate loans [54]. The median debt ratio of the petroleum refining industry was 56% in the U.S. in 2019 [55]. As production of MTO-MOGD fuels relies on novel technologies and has a higher financial risk, a debt ratio of 70% was assumed in the calculations. A 6% cost of equity was found to be reasonable when considering the small scale of the production plant. It was decided to neglect taxes as they would be paid by the company owning the plant.

Table 2. Prices of the raw materials, products, consumables, and utilities. The prices of methanol, hydrogen, and electricity were chosen based on their renewable origin.

	Unit	Value	Reference
Exchange rate	USD/€	0.84	25.11.2020
Methanol	€/t	963	[56]
Hydrogen	€/kg	3.00	[56]
Ni/γ-Alumina catalyst	€/kg	13.4	[57]
ZSM-5 catalyst	€/kg	8.40	[58]
Gasoline	€/t	1196	[35,59]
Kerosene	€/t	1171	[35,59]
Diesel	€/t	1143	[35,59]
LPG	€/t	551	[60]
Steam	€/t	30	[60]
Wastewater	€/t	0.72	[61]
Cooling water	€/t	0.17	[62]
Electricity	€/MWh	39.6	[60]

Table 3. Assumptions made for calculating plant profitability.

Cost Species	Basis
Working capital	5% of TFCC
Number of shifts	4.8
Number of operators per shift	5
Salary per operator	40,000 €/a
Supervision	25% of operating labour
Direct overhead	50% of operating labour and supervision
Maintenance	3% of ISBL
Plant overhead	65% of labour and maintenance
Insurance	1% of TFCC
Plant lifetime	20 a
Annual operation time	8000 h
Debt ratio	70%
Interest rate	2%
Cost of equity	6%
Tax rate	0%

Catalysts prices were estimated from foreign bulk order prices by including service fees from shipping, customs, and installation. The total price was determined by multiplying the bulk price by a factor of two to consider additional costs related to the acquisition of the catalysts. Prices of the fuel products were assumed to consist of the price of each fossil fuel and a premium price related to CO_2 emission reduction. A premium of 350 €/t, which is the highest price in the current European market [59], was considered for each fuel product. Such fuel pricing would create competition between synthetic and biofuels in the low-emission fuel markets.

3. Results and Discussion

3.1. Simulation Results

Mass balance and hydrocarbon yields of the product streams calculated from the simulation results are listed in Table 4. A complete stream table can be found in the Supplementary Materials.

Table 4. Mass balance and hydrocarbon yields of the model and in the reported literature [22].

Fraction	Stream Type	Stream Number	Mass Flow, kg/h	Calculated Hydrocarbon Yield, wt%	Reference Hydrocarbon Yield, wt%
Methanol	Inlet	1	3000	-	-
Hydrogen	Inlet	64	0.19	-	-
Hydrogen	Inlet	66	7.17	-	-
Gasoline	Outlet	30	224	17	15
Diesel	Outlet	53	591	45	57
Kerosene	Outlet	55	356	27	25
Purge 1	Outlet	56	1.43	-	-
Water	Outlet	69	1679	-	-
Fuel gas	Outlet	70	98.1	7.4	1.0
Purge 2	Outlet	71	0.04	-	-
LPG	Outlet	72	59.1	4.5	2.0
Total				100	100

The design of the model was based on the experimental work reported by Avidan [22], and the hydrocarbon yield structures in Table 4 correspond relatively well to the reference values. The surplus of fuel gas and LPG approximately cover the deficiency in diesel yield compared with the reference. As discussed above, the light compounds contribute to the formation of heavier hydrocarbon compounds. The yield structure indicates that the

conversion in both the MTO and MOGD reactors R-101 and R-103, respectively, should be directed towards longer carbon chains.

Next, the utility consumption of the process shown in Table 5 is addressed. As the design principle was based on heat integration within the model, the heating requirements in the reactor pre-heaters and distillation reboiler can be covered by the internal steam and fired heat production. Cooling of the exothermic reaction heat and the relatively high operation temperatures lead to a net surplus production of LP and HP steam. The residual cooling demand is covered by cooling water, which is the largest individual utility consumption. The electricity demand of the process is rather small, and the integration of excess LP steam production for electricity generation can be considered. Energy savings of 20.8 MW and 1.2 M€ per annum are achieved by the suggested heat integration including fuel gas combustion.

Table 5. Utility consumption of the MTO-MOGD process. Positive duty values indicate utility inputs and negative values utility generation.

	Utility	kW	kWh/t_{fuels}	t/t_{fuels}
Consumption	Refrigerant	39	33	-
	Cooling water	732	626	108
	LP steam	52	44	0.1
	HP steam	302	259	0.5
	Fired heat	452	386	2.3
	Electricity	75	64	-
Generation	LP steam	−569	−486	0.8
	HP steam	−1355	−1158	2.4
	Fired heat	−1095	−936	-
Total demand	Cooling	771	659	108
	Heating	806	689	2.9
	Electricity	114	98	-
	Steam	−2213	−1891	−0.3

The properties of the modelled gasoline, kerosene, and diesel are compared with directive 2009/30/EC and standard ASTM D1655 in Table 6. An elevated olefin content indicates that the gasoline fraction requires hydrogenation in a manner similar to kerosene and diesel cuts. The diesel properties are within the guideline values, while kerosene is at the lower end of the quality standards, with only the aromatic content and 10 vol% distillation recovery temperature being within the target values. The hydrocarbon distribution of kerosene was also the most simplified because kerosene is estimated to consist solely of C_{12} compounds.

As fuels produced in the simulated process do not comply with the quality requirements, further treatment of the fuel cuts is needed for sale as drop-in products. For the case of gasoline, increasing the research octane number (RON) to realise a value of 95 is required. The RON can be adjusted to the required levels via straightforward methanol/ethanol blending. Additionally, the benzene content of the gasoline must be significantly reduced since it is markedly higher than the maximum allowable concentration. Kerosene requires more comprehensive treatment to adjust the quality to the standard for aviation fuel. If the MTO-MOGD plant is owned by a company with an established position in fuel production and distribution, it might be worthwhile to refine the raw fuel cuts at an existing fuel refinery with adequate process technology and the necessary additive chemicals.

Table 6. Modelled fuel properties in comparison to the minimum and maximum values in directive 2009/30/EC and standard ASTM D1655 [63–66]. In the table, FAME refers to fatty acid methyl esters.

Specification	Unit	Gasoline	Kerosene	Diesel	Quality Minimum	Quality Maximum
Research octane number		89			95	-
Reid vapor pressure	kPa	95			-	60
Density at 15 °C	kg/m^3		668		775	840
	kg/m^3			890	-	845
Flash point	°C	−64			−40	-
	°C		−2		38	-
	°C			113	60	-
10 vol% recovery	°C		92		-	205
95 vol% recovery	°C			329	-	360
Final boiling point	°C		316		-	300
Olefins	vol%	21			-	18
Aromatics	vol%	23			-	35
	vol%		8		-	25
Benzene	vol%	13			-	1
Polycyclic aromatics	wt%			0	-	8
Oxygen	wt%	2.9		0	0	3.7
Methanol	vol%	0			0	3
FAME	vol%			0	-	7
Sulphur	mg/kg	0			-	10
Lead	mg/L	0			-	5

3.2. Thermodynamic Model Comparison

Table 7 summarises a comparison of the PENG-ROB model with the other tested property models. It can be seen that there are no significant differences in the results as predicted by PENG-ROB, PR-BM, and SRK, justifying the use of any of these methods for modelling the present process. Both the PENG-ROB and SRK methods (also with the Boston–Matthias modification) are commonly used for modelling similar processes incorporating syngas, methanol, and hydrocarbon processing [60,67,68]. A more significant deviation was found with the RKSMHV2 method, which appears to rule out its use for this process pending a more detailed analysis. Based on this analysis, the use of the PENG-ROB property method was considered acceptable.

Table 7. Comparison of the tested Aspen Plus property methods in terms of the relative differences in product fraction mass flow rates compared to the PENG-ROB model.

Property Method	PENG-ROB	PR-BM	SRK	RKSMHV2
Gasoline flow rate	0.0%	−0.1%	0.5%	−1.5%
Diesel flow rate	0.0%	1.2%	0.1%	8.9%
Kerosene flow rate	0.0%	−2.1%	−0.6%	−16.0%
LPG flow rate	0.0%	0.3%	−0.6%	−6.2%

3.3. Economic Analysis

The equipment type, size, and cost are listed in the Supplementary Materials. The division of the purchased equipment cost per component type is illustrated in Figure 6.

Figure 6 shows that over 75% of the total equipment cost is covered by the compressors, and the rest of the components account for the remaining quarter, among which the reactors and distillation columns are the most expensive.

The structure of total fixed capital cost of the MTO-MOGD plant is shown in Table 8. The purchased equipment charges are a rather small portion of the total fixed capital expenditure once the other complementary costs are taken into account. In particular,

design and engineering make up a large portion of the investment. This type of capital cost calculation can be considered as an initial order of magnitude estimate.

	Comp	Dec	Dist	HeatX	Flash	Pumps	Reac	Total
M€	5.17	0.02	0.39	0.24	0.08	0.16	0.76	6.82
%	76%	0.2 %	6%	4%	1%	2%	11%	100%
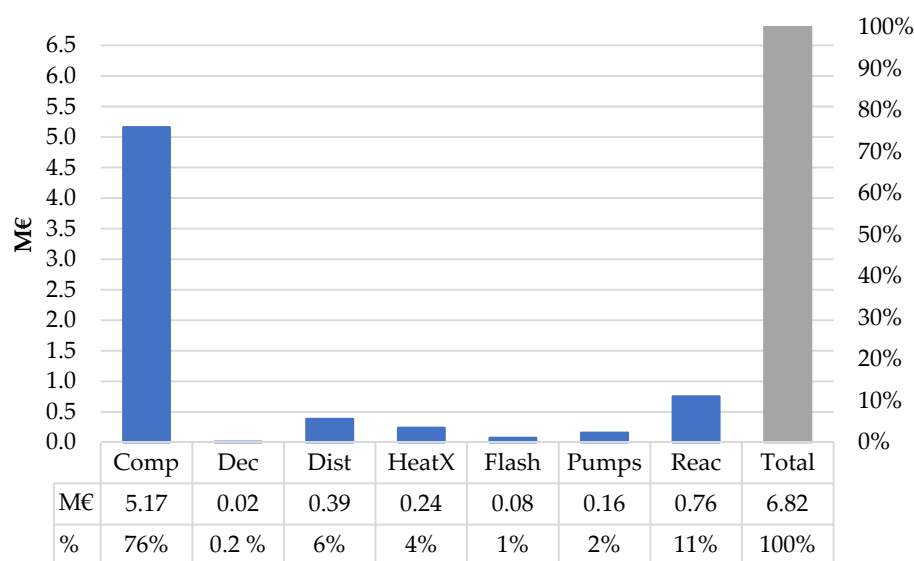
Figure 6. Cost structure of purchased equipment. Abbreviations in the figure: Comp, compressors; Dec, decanters; Dist, distillation columns; HeatX, heat exchangers; Flash, flash columns; Reac, reactors.

Figure 6 shows that over 75% of the total equipment cost is covered by the compressors, and the rest of the components account for the remaining quarter, among which the reactors and distillation columns are the most expensive.

The structure of total fixed capital cost of the MTO-MOGD plant is shown in Table 8. The purchased equipment charges are a rather small portion of the total fixed capital expenditure once the other complementary costs are taken into account. In particular, design and engineering make up a large portion of the investment. This type of capital cost calculation can be considered as an initial order of magnitude estimate.

Table 8. Fixed capital cost structure of the MTO-MOGD plant.

Cost Species	Basis	M€
Major equipment purchase cost	Major equipment sizing	6.82
ISBL investment	Equation (5) and Table 1	24.7
OSBL cost	40% of ISBL	9.87
Design & engineering	30% of ISBL and OSBL	10.4
Contingency	10% of ISBL and OSBL	3.45
Total fixed capital cost	Equation (6)	48.4

Table 9 breaks down the charges forming the total cost of production. Figure 7 shows how the different operational charges contribute to the total annual costs. The catalyst cost is based on the specific total catalyst consumption of 0.34 kg/t_{fuels} and a 2-year catalyst lifetime.

Table 9. Breakdown of the production costs of synthetic fuels. Sales of the by-product LPG and excess steam are included in the VCOP.

Cost Species	M€/a	€/t_{fuels}	% of TCOP
VCOP	23.2	2479	73
FCOP	5.75	614	18
ACC	2.96	316	9
TCOP	31.9	3409	100

M€/a	MeOH	H2	Cat	WW	Elec	CW	Lab	Maint	Ovhd	ACC	Sales	Total
M€/a	23.1	0.18	0.03	0.01	0.04	0.18	1.74	1.45	2.56	2.96	0.33	31.9
%	72%	0.6 %	0%	0.0 %	0.1 %	1%	5%	5%	8%	9%	1%	100%
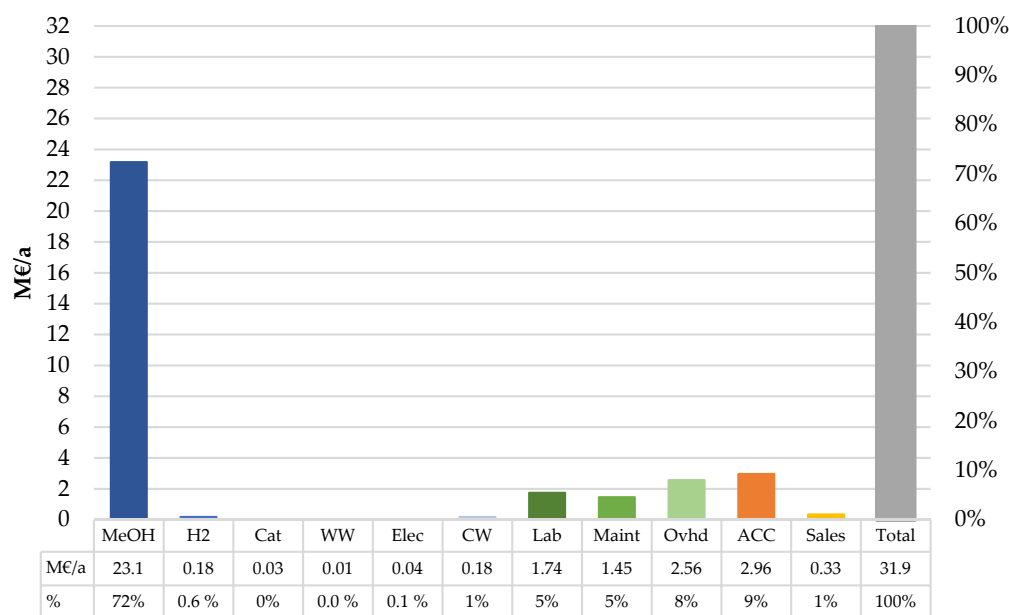
Figure 7. Breakdown of annual operational expenses and annualised capital charge. Variable operating costs are indicated with blue colours, fixed operating costs with green shades, and annualised capital charge with orange. Abbreviations in the figure: Cat, catalysts; WW, wastewater; Elec, electricity; CW, cooling water; Lab, labour; Maint, maintenance; Ovhd, overheads; ACC, annualised capital charge. Sales of the by-product LPG and excess steam are included in the figure in yellow, but they are not accounted for in the total costs.

It is evident in Table 9 and Figure 7 that the variable cost of production (VCOP) accounts for the major portion of the total cost of production (TCOP). The VCOP is heavily dependent on the methanol price as methanol accounts for ~70% of the annual costs. An important factor affecting the methanol consumption is the reaction stoichiometry. According to Equations (1) and (2), water is split from methanol in an equimolar ratio, leading to the loss of hydrogen in the form of water. The mass efficiency of methanol to fuels (39%) therefore results in a further increase in the cost of methanol from 963 €/t to the final production cost of 2470 €/t$_{fuels}$. In turn, the methanol price largely depends on the price of renewable electricity used for hydrogen production via electrolysis. Nieminen et al. [56] calculated that hydrogen accounts for ~90% of the variable cost of methanol production and 70% of total fixed capital cost. A more detailed breakdown of the methanol production costs was presented by Nieminen et al. [56]. As a result of the high dependency on the methanol price, the TCOP of 3409 €/t$_{fuels}$ is also considerably higher than the average fuel product price of 1170 €/t used for the profitability calculations. A re-evaluation of the product price is therefore required to find the break-even point for the investment.

3.4. Sensitivity Analysis

3.4.1. Component Selection

Sensitivity analysis was carried out to study the effect of increasing the number of key components describing the kerosene fraction. The effect of adding C_{10} and C_{14} compounds to the fraction was evaluated by comparing the energy consumption figures in the distillation column DIST4 where kerosene is separated from diesel. In the analysis, C_{12} kerosene was considered as the benchmark. C_{10} and C_{14} normal and branched paraffins and 1-olefins were included in the distillate feed with the mass fractions of the corresponding C_{12} compounds. The total amount of kerosene was kept constant in all cases. It was assumed that the distillate mixture enters the distillation column at 100 °C and atmospheric pressure. A partial condenser was used to produce vapour distillate. The results of the sensitivity analysis are illustrated in Figure 8.
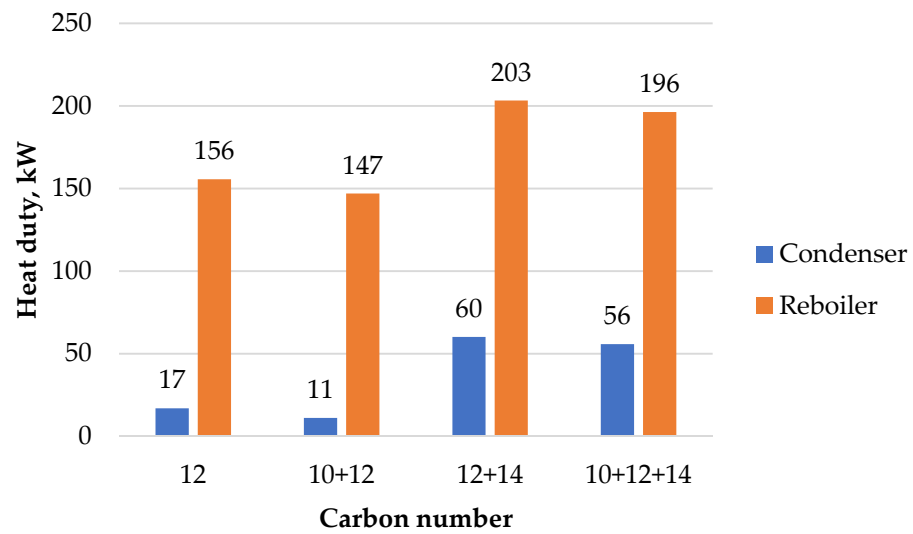
Figure 8. Sensitivity analysis on the effect of the number of kerosene compounds to required duty for separation of kerosene and diesel.

Figure 6 shows that neither the required condenser nor the reboiler duty changes notably, even if the composition of the kerosene was altered towards lighter hydrocarbons. The addition of C_{14} compounds increases the reboiler and condenser duties by 23% and 72%, respectively. The results are logical for lowering the average molar mass of the mixture would lead to less laborious separation of kerosene from diesel. Correspondingly, increasing the carbon number in the kerosene fraction decreases the boiling point difference of the fuels because the C_{16} compounds represent the lower limit of the diesel fraction.

Based on these findings, the number of compounds present in the carbon number distribution are less significant than the actual components. It might be possible to improve the ability of the model to describe the fuels via proper selection of the key components representing the fractions. The specification between paraffins and olefins and their different isomers is probably the most important factor affecting the performance of the separation stages and ultimately the product properties.

3.4.2. Profitability

The economics of the plant was inspected in further detail via sensitivity analysis. As discussed in the previous section, the selected fuel price is not in line with the calculated cost of production. Sensitivity analysis was carried out to investigate various options to improve the production profitability. The total capital expenditure (CAPEX) and methanol price were selected for investigation against the net present value (NPV). The results of the analysis for both variables are illustrated in Figures 9 and 10. Complementary descriptions of the methanol prices in Figure 10 are listed in Table 10.
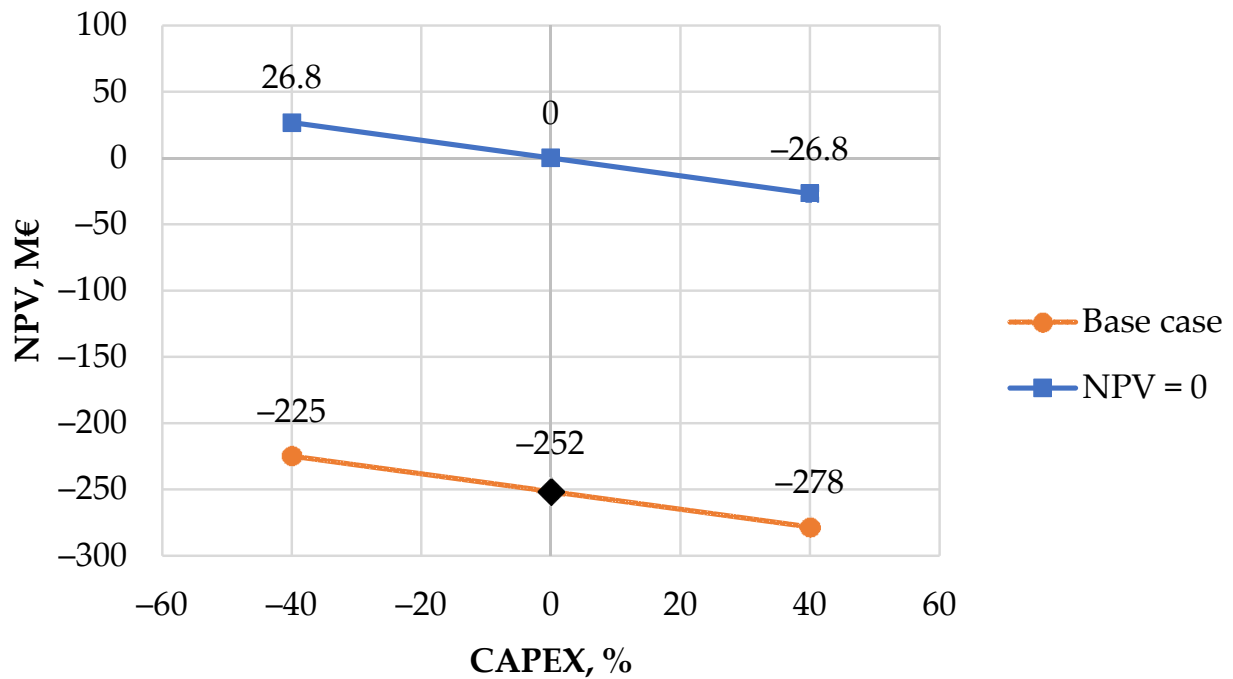
Figure 9. Effect of capital expenditure (CAPEX) on net present value (NPV) over the 20-year plant lifetime and 2% interest rate. Black diamond indicates the starting point of the analysis with methanol price of 963 €/t and average fuel price of 1170 €/t. Point (0,0) is achieved by increasing the fuel price to 3208 €/t while keeping other values constant.
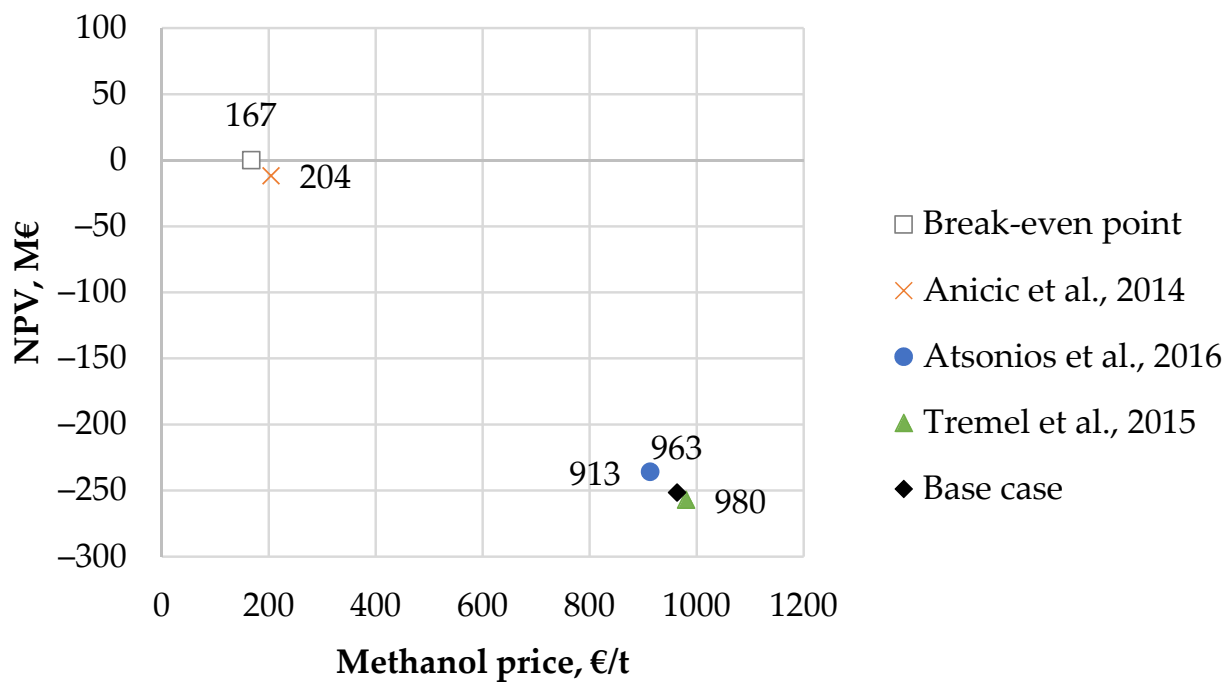
Figure 10. Effect of methanol price on net present value (NPV) over the 20-year plant lifetime and 2% interest rate. Black diamond indicates the base case with methanol price of 963 €/t and average fuel price of 1170 €/t. The white square represents the break-even point with a constant fuel price.

Table 10. Prices of high purity methanol ($\geq$99.2 wt%) reported in the literature. Hydrogen prices were calculated based on the electricity price if not specified in the reference.

Reference	MeOH, €/t	H$_2$, €/kg	Electricity, €$_{2015}$/MWh	Notes
Anicic et al. [69]	204	2.11	39.6 [1]	Hydrogen from electrolysis.
Atsonios et al. [70]	913	2.49	51.5	Hydrogen from alkaline electrolysis.
Nieminen et al. [56]	963	3.00	57.5	Hydrogen from alkaline electrolysis. The price includes costs of hydrogen production and storage. The electrolysis is powered by 30 MW of wind electricity.
Tremel et al. [71]	980	3.00	93.0	Hydrogen from PEM electrolysis. The price includes hydrogen production, storage, and transport costs.

[1] Electricity price according to Hannula (2015) [60].

Variation of CAPEX by either -40% or $+40\%$ was considered in the analysis. The case of -40% can be realised in a situation where the synthetic fuel plant is granted the maximum investment subsidy from the Ministry of Economic Affairs and Employment of Finland. These investment aids are provided for projects that aim at investing in novel technologies in the field of sustainable and renewable energy production [72].

The sensitivity analysis of individual variables shows that investment subsidy alone would not improve the NPV with a fuel price of 1170 €/t. The subsidy would increase the NPV to 27 M€ if the fuel was priced at 3208 €/t. On the other hand, the NPV is strongly dependent on the methanol price and the NPV rapidly increases with decreasing methanol price, but the break-even point for the investment can be achieved at methanol prices lower than those from comparable literature studies.

Although hydrogen consumption during the production process is low as a result of the high level of recycling, the cost of hydrogen would influence the profitability of the synthetic fuel plant via the methanol production cost. The price of hydrogen currently varies between 1.50 and 2.50 €/kg [50,73] depending on the production method. The lowest cost can be achieved using natural gas as the hydrogen source for steam methane reforming, while the higher values are associated with the conversion of electricity into hydrogen via the electrolysis of water. The cost of electrolytic hydrogen production is directly proportional to the price of electricity, and water electrolysis is viewed as one of the most interesting technologies for producing green hydrogen with renewable electricity.

An alternative scenario to fossil or electrolytic hydrogen would be hydrogen that is available from the chemical industry as an underutilised by-product. These types of point sources of hydrogen include, for instance, chlorate production for pulp bleaching purposes. By-product hydrogen can generally be considered less expensive than hydrogen produced via water electrolysis. A lower cost of hydrogen would first enable small-scale production of renewable synthetic fuels taking into consideration the limited availability of hydrogen as an industrial side stream. Large-scale production could be realised on decreasing the cost of renewable electricity, which would lead to decreased hydrogen and methanol costs. Additionally, valuable operational experience would be gained by operating the plants first at the pilot and demonstration scales.

Because synthetic fuel production via MTO-MOGD does not appear to be economically attractive in light of the figures, sensitivity analysis was carried out from an alternate perspective. The investigation was carried out using the same variables as the previous analysis, and their effects on the production cost were evaluated. The product prices were increased so that the NPV reaches zero at the end of the plant lifetime. The results of the analysis are shown in Figure 9. The fuel production cost in Figure 11 is considered as an average of the three fuels, taking the different fuel densities into account.
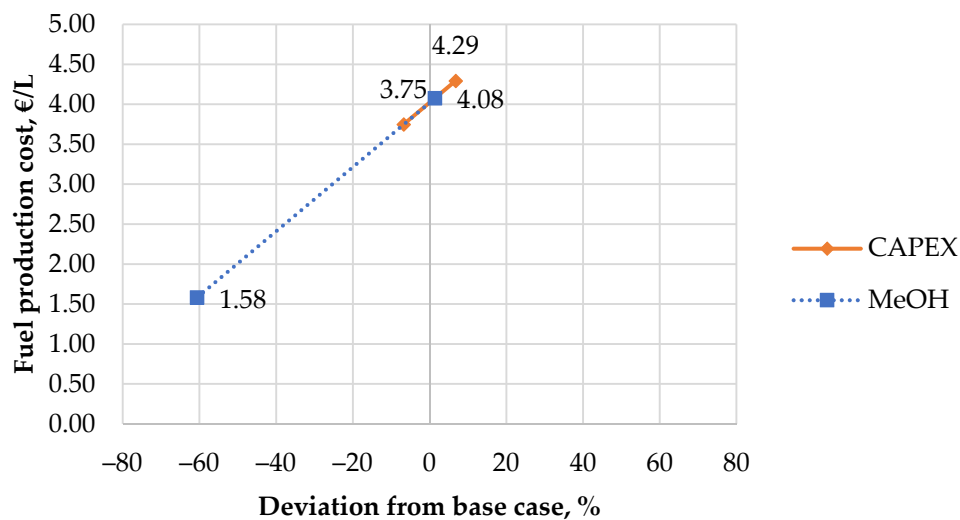
Figure 11. Sensitivity analysis for the average fuel production cost when the net present value over the 20-year plant lifetime and the 2% interest rate is set to zero by increasing the average fuel price to 3208 €/t while the methanol price is maintained at 963 €/t.

It is clear that the cost of methanol is the most significant factor affecting the fuel price. The production cost of renewable methanol is highly dependent on the cost of electrolytic hydrogen, which in turn depends on the price of electricity and the rather limited electrolysis efficiency. The most remarkable cost reduction potential in methanol production lies in the use of industrial by-product hydrogen, while the price of renewable electricity continues to decline and the efficiency of power conversion to hydrogen is further increased. CO_2 capture also accounts for a share of the production costs, but it has minor significance compared with hydrogen production.

A lower methanol price or higher final product prices would significantly improve the profitability of the plant. The pay-back time of the investment is 14.2 years, and the internal rate of return is 3.2% when the break-even point is realised by the end of the plant lifetime. Such a situation can be achieved with a methanol price of 167 €/t or average fuel production cost of 4.02 €/L (3208 €/t).

Table 11 shows a cost comparison for the fossil and renewable fuels considered in this work. The price of fossil methanol is the European market price [74]. The energy content of fossil and biofuel blend is calculated as a weighted average by assuming that 18% of the total energy content of the mixture is covered by the biofuel component, as set in the Finnish biofuel distribution mandate for 2021 [75]. Table 11 shows that there is a 100 €/MWh price difference between fossil and PTL methanol, making renewable methanol 150% more expensive. The difference is even larger when comparing the fossil/biofuel blend to MTO-MOGD products. The price of MTO-MOGD fuels is ~270 €/MWh, which is nearly three-fold higher compared with the fuel blend. Using the price of fossil methanol instead of PTL would decrease the TCOP of MTO-MOGD products to 155 €/MWh. This demonstrates the significance of methanol pricing once again.

Table 11. Prices of fossil and PTL fuels on mass and lower heating value (LHV) basis. Gasoline, kerosene, and diesel are considered via average LHVs and prices. The price per ton of MTO-MOGD fuels is the calculated TCOP.

Fuel Type	MJ/kg	€/t	€/GJ	€/MWh	Reference
Fossil MeOH	19.9	390	19.6	70.6	[74,76]
PTL MeOH	19.9	963	48.4	174	[56,59]
Fossil transport fuels	43.0	820	19.1	68.6	[35,76]
Fossil/biofuel blend	43.2	1170	27.1	97.4	[35,59,75]
MTO-MOGD fuels	45.0	3409	75.7	273	This work

3.5. Further Discussion

Biofuel quotas are a practical implication of the emission reduction targets for the transport sector set in the recast Renewable Energy Directive 2018/2001/EU (RED II) [77]. Fulfilment of the distribution obligation is controlled by setting a penalty to which the distributing company is subject to if it fails to meet the obligation [78]. Transport fuel premiums or emission reduction tickets are tradeable certificates indicating the amount of CO_2 equivalents avoided by replacing a portion of the fossil fuels with biofuels [79]. Fuel suppliers can therefore either invest in biofuel production and sell the excess certificates or buy tickets from another distributor to fulfil their mandates. As the share of low-carbon fuels in the distributed fuel mixture increases over time, biofuels will not be adequate as the sole contributor for fulfilling the mandates. In particular, restrictions on the use of first-generation biofuels, the risks of indirect land-use change, and the limited availability of advanced biofuels put pressure on fuel distribution companies.

Renewable synthetic transport fuels are not yet recognised as an option for fulfilling the distribution obligation in Finnish legislation. However, a government proposal of including renewable fuels of non-biological origin in the national legislation as an implication of RED II is currently pending [80]. The current and pending legislation in Finland includes only road transport in the CO_2 emission reduction schemes, even though road transport can be converted more readily to electric than maritime transport or aviation. Thus, only a portion of transport-related emissions can be reduced. Comprehensive regulation considering all three forms of motor transport would be necessary to decarbonise the entire transport sector. Obligatory regulation with a blending mandate for both biofuels and synthetic fuels would also create competition for biofuel blends on the markets. Hence, policy support is recognised as a necessity to motivate energy companies to invest in sustainable fuel technology that presently have unfavourable economics [81].

Sustainability issues related to biofuels and strict articles of RED II considering PTL fuels could be avoided in a pulp mill environment. In addition to pulp, mills convert biomass into biogenic CO_2 and renewable steam and electricity. There is excellent potential for synthetic fuel production because every process step can be carried out on-site. Carbon emissions could be turned into a raw material via CO_2 capture. Excess electricity could be used to power green hydrogen production instead of feeding it to a municipal power grid. Methanol forming in kraft pulping as a by-product could also be used to boost MeOH production from CO_2 and H_2. The forest industry is one of the largest industry sectors in Finland, thus offering an ideal platform for integrated bioproduct and carbon-neutral transport fuel production.

4. Conclusions

A simulation model of transport fuel production via the MTO and MOGD processes was created using Aspen Plus. The performance of the model in terms of product quantities was investigated by comparing physical property estimation methods, and an economic analysis of the combined process was carried out based on the model. The profitability analysis showed that the plant is not profitable with a renewable methanol price of 963 €/t and an average premium fuel price of 1170 €/t. Methanol was observed to impact the profitability of the plant the most in terms of the stoichiometric loss of hydrogen as water and the high production cost of PTL methanol. It was calculated that the average product price should be 3208 €/t at the given methanol price to realise a break-even point at the end of the 20-year plant lifetime. The results clearly demonstrate that synthetic fuels with a production cost of 3409 €/t cannot compete in markets dominated by inexpensive fossil fuels without regulatory incentives. Nonetheless, it is worth noting that the economic results are indicative as the simulation model is not fully optimised and validated by conventional means. The uncertainties related to unfinished regulation in RED II also slow down necessary investments in PTL technology. As the goal of the EU and Finland is decarbonisation of the transport sector, the indirect use of green hydrogen in synthetic fuel production should not be limited or hindered in any way. Therefore, the future practical adoption

of alternative liquid transport fuel production methods, such as via the MTO-MOGD process presented herein, should be promoted via the provision of moderate incentives, tax exemptions, and allocating a monetary burden on carbon-intensive processes.

Supplementary Materials: The following are available online at https://www.mdpi.com/article/10.3390/pr9061046/s1. Table S1: Component specifications of the MTO-MOGD model. Table S2: Reaction specifications of the MTO reactor R-101 and standard reaction enthalpies calculated from literature values and estimated by Aspen Plus. Table S3: Reaction specifications of the hydroisomerisation reactor R-102. Table S4: Reaction specifications of the MOGD reactor R-103 and standard reaction enthalpies calculated from literature values and estimated by Aspen Plus. Table S5: Reaction specifications of the hydrogenation reactor R-104. Table S6: Equipment specifications of the MTO-MOGD model. Table S7: Equipment sizes and costs. Table S8: Stream table of the MTO-MOGD model.

Author Contributions: J.R., A.L., T.K., and P.L. conceptualised and designed this work. J.R. and H.N. created the simulation model. J.R. and A.R.D. performed formal data analysis based on the model. A.L., T.K., P.L., A.V., and M.H. supervised the research. All authors have read and agreed to the published version of the manuscript.

Institutional Review Board Statement: Not applicable.

Informed Consent Statement: Not applicable.

Data Availability Statement: Data is contained within the article and the Supplementary Materials.

Conflicts of Interest: The authors declare no conflict of interest.

Nomenclature

ACC	Annual capital charge
APEA	Aspen Process Economic Analyzer
CAPEX	Capital expenditure
COD	Conversion of Olefins to Distillate
CS	Carbon steel
DME	Dimethyl ether
EU	European Union
FAME	Fatty acid methyl esters
FCOP	Fixed cost of production
FT	Fischer–Tropsch
HP	High-pressure
ISBL	Inside battery limits
LHV	Lower heating value
LP	Low-pressure
LPG	Liquefied petroleum gas
MeOH	Methanol
MOGD	Mobil's Olefins to Gasoline and Distillate
MTG	Methanol-to-gasoline
MTO	Methanol-to-olefins
NPV	Net present value
OSBL	Outside battery limits
PENG-ROB	Peng–Robinson
PR-BM	Peng–Robinson–Boston–Mathias
PetroSA	The Petroleum Oil and Gas Corporation of South Africa
PTL	Power-to-liquid
RED II	Recast Renewable Energy Directive 2018/2001/EU
RKSMHV2	Redlich–Kwong–Soave–Huron–Vidal
RON	Research octane number

SRK	Soave–Redlich–Kwong
TIGAS	Topsøe Integrated Gasoline Synthesis
TRL	Technology readiness level
TCOP	Total cost of production
VCOP	Variable cost of production
C	Cost, €
DE	Design & engineering, %
f	Correction factor
$\dot{m}$	Mass flow rate, kg/s
OS	OSBL cost, %
X	Contingency, %
c	Civil work
e	Equipment
el	Electrical
er	Equipment erection
ic	Instrumentation and control
l	Lagging and paint
m	Material
p	Piping
s	Structures and buildings
TFCC	Total fixed capital cost

References

1. The Paris Agreement. Available online: https://unfccc.int/files/essential_background/convention/application/pdf/english_paris_agreement.pdf (accessed on 16 October 2020).
2. 2050 Long-Term Strategy. Available online: https://ec.europa.eu/clima/policies/strategies/2050_en (accessed on 16 October 2020).
3. Coalition-McKinsey, E.U. *A Portfolio of Power-Trains for Europe: A Fact-Based Analysis-The Role of Battery Electric Vehicles, Plug-In Hybrids and Fuel Cell Electric Vehicles*; European Union: Brussels, Belgium, 2010.
4. Weil, M.; Ziemann, S.; Peters, J. The Issue of Metal Resources in Li-Ion Batteries for Electric Vehicles. In *Behaviour of Lithium-Ion Batteries in Electric Vehicles: Battery Health, Performance, Safety, and Cost*; Springer: Berlin/Heidelberg, Germany, 2018; pp. 59–74.
5. European Automobile Manufacturers' Association (ACEA). *Vehicles in Use*; ACEA: Brussels, Belgium, 2021.
6. Announced Wind and Solar PV Average Auction Prices by Commissioning Date, 2012–2020. Available online: https://www.iea.org/data-and-statistics/charts/announced-wind-and-solar-pv-average-auction-prices-by-commissioning-date-2012-2020 (accessed on 11 March 2021).
7. Moller, A.P. Maersk Will Operate the World's First Carbon Neutral Liner Vessel by 2023—Seven Years Ahead of Schedule. Available online: https://www.maersk.com/news/articles/2021/02/17/maersk-first-carbon-neutral-liner-vessel-by-2023 (accessed on 18 February 2021).
8. Becker, W.L.; Penev, M.; Braun, R.J. Production of Synthetic Natural Gas from Carbon Dioxide and Renewably Generated Hydrogen: A Techno-Economic Analysis of a Power-to-Gas Strategy. *J. Energy Resour. Technol.* **2019**, *141*, 021901. [CrossRef]
9. Wang, J.; Wang, H.; Fan, Y. Techno-Economic Challenges of Fuel Cell Commercialization. *Engineering* **2018**, *4*, 352–360. [CrossRef]
10. Dieterich, V.; Buttler, A.; Hanel, A.; Spliethoff, H.; Fendt, S. Power-to-liquid via synthesis of methanol, DME or Fischer–Tropsch-fuels: A review. *Energy Environ. Sci.* **2020**, *13*, 3207–3252. [CrossRef]
11. Boyd, R. Climate Change Mitigation. In *2019 Environmental Report: Aviation and Environment*; ICAO: Montreal, QC, Canada, 2019; pp. 174–176.
12. Lufthansa Will Buy Green Kerosene from Northern German Refinery. Available online: https://www.cleanenergywire.org/news/lufthansa-will-buy-green-kerosene-northern-german-refinery (accessed on 27 January 2021).
13. Transforming Waste into Sustainable Advanced Biofuels. Available online: https://www.altalto.com (accessed on 27 January 2021).
14. Total Fuel Consumption of Commercial Airlines Worldwide between 2005 and 2021. Available online: https://www.statista.com/statistics/655057/fuel-consumption-of-airlines-worldwide (accessed on 29 January 2021).
15. Speight, J. *Synthetic Fuels Handbook: Properties, Process, and Performance*; McGraw-Hill: New York, NY, USA, 2008.
16. Schmidt, P.; Weindorf, W.; Roth, A.; Batteiger, V.; Riegel, F. *Power-to-Liquids: Potentials and Perspectives for the Future Supply of Renewable Aviation Fuel*; German Environment Agency: Dessau-Roßlau, Germany, 2016.
17. Van der Burgt, M.; van Leeuwen, C.; del'Amico, J.; Sie, S. The Shell Middle Distillate Synthesis Process. In *Methane Conversion*; Bibby, D., Chang, C., Howe, R., Yurchak, S., Eds.; Elsevier Science Publishers: Amsterdam, The Netherlands, 1988; Volume 36, pp. 473–482.
18. Knottenbelt, C. Mossgas "gas-to-liquid" diesel fuels—An environmentally friendly option. *Catal. Today* **2002**, *71*, 437–445. [CrossRef]

19. COD Technology. Available online: http://www.petrosa.co.za/innovation_in_action/Pages/COD-Technology.aspx (accessed on 14 December 2020).

20. Yurchak, S. Development of Mobil's Fixed-Bed Methanol-to-Gasoline (MTG) Process. In *Methane Conversion*; Bibby, D., Chang, C., Howe, R., Yurchak, S., Eds.; Elsevier Science Publishers: Amsterdam, The Netherlands, 1988; Volume 36, pp. 251–272.

21. Topp-Jørgensen, J. Topsøe Integrated Gasoline Synthesis—The TIGAS Process. In *Methane Conversion*; Bibby, D., Chang, C., Howe, R., Yurchak, S., Eds.; Elsevier Science Publishers: Amsterdam, The Netherlands, 1988; Volume 36, pp. 293–305.

22. Avidan, A. Gasoline and Distillate Fuels from Methanol. In *Methane Conversion*; Bibby, D., Chang, C., Howe, R., Yurchak, S., Eds.; Elsevier Science Publishers: Amsterdam, The Netherlands, 1988; Volume 36, pp. 307–323.

23. Tabak, S.; Yurchack, S. Conversion of methanol over ZSM-5 to fuels and chemicals. *Catal. Today* **1990**, *6*, 307–327. [CrossRef]

24. Olah, G. CO_2 to Renewable Methanol Plant, Reykjanes. Available online: https://www.chemicals-technology.com/projects/george-olah-renewable-methanol-plant-iceland (accessed on 23 October 2020).

25. Grimmer, H.; Nitschke, E.; Thiagarajan, N. Conversion of Methanol to Liquid Fuels by the Fluid Bed Mobil Process (A commercial concept). In *Methane Conversion*; Bibby, D., Chang, C., Howe, R., Yurchak, S., Eds.; Elsevier Science Publishers: Amsterdam, The Netherlands, 1988; Volume 36, pp. 273–291.

26. Stöcker, M. Methanol-to-hydrocarbons: Catalytic materials and their behavior. *Microporous Mesoporous Mater.* **1999**, *29*, 3–48. [CrossRef]

27. Schmidt, P.; Zittel, W.; Weindorf, W.; Raksha, T. *Renewables in Transport 2050—Empowering a Sustainable Mobility Future with Zero Emission Fuels from Renewable Electricity*; Ludwig Bölkow Systemtechnik GmbH (LBST): Frankfurt, Germany, 2016.

28. Dahl, I.M.; Kolboe, S. On the Reaction Mechanism for Hydrocarbon Formation from Methanol over SAPO-34. *J. Catal.* **1996**, *161*, 304–309. [CrossRef]

29. NIST Chemistry WebBook. Available online: https://webbook.nist.gov/chemistry (accessed on 26 February 2021).

30. Cheméo: High Quality Chemical Properties. Available online: https://www.chemeo.com (accessed on 26 February 2021).

31. Mokrani, T.; Scurrel, M. Gas Conversion to Liquid Fuels and Chemicals: The Methanol Route-Catalysis and Processes. *Catal. Rev.* **2009**, *51*, 1–145. [CrossRef]

32. Keil, F.J. Methanol-to-hydrocarbons: Process technology. *Microporous Mesoporous Mater.* **1999**, *29*, 49–66. [CrossRef]

33. Baliban, R.C.; Elia, J.A.; Weekman, V.; Floudas, C.A. Process synthesis of hybrid coal, biomass, and natural gas to liquids via Fischer–Tropsch synthesis, ZSM-5 catalytic conversion, methanol synthesis, methanol-to-gasoline, and methanol-to-olefins/distillate technologies. *Comput. Chem. Eng.* **2012**, *47*, 29–56. [CrossRef]

34. Baliban, R.; Elia, J.; Floudas, C. Biomass to liquid transportation fuels (BTL) systems: Process synthesis and global optimization framework. *Energy Environ. Sci.* **2013**, *6*, 267–287. [CrossRef]

35. Onel, O.; Niziolek, A.M.; Elia, J.A.; Baliban, R.C.; Floudas, C.A. Biomass and Natural Gas to Liquid Transportation Fuels and Olefins (BGTL+C2_C4): Process Synthesis and Global Optimization. *Ind. Eng. Chem. Res.* **2014**, *54*, 359–385. [CrossRef]

36. Aspen Technology, Inc. *Aspen Physical Property System. Physical Property Methods V8.4*; Aspen Technology: Burlington, MA, USA, 2013.

37. Shi, C.; Elgarni, M.; Mahinpey, N. Process design and simulation study: CO_2 utilization through mixed reforming of methane for methanol synthesis. *Chem. Eng. Sci.* **2021**, *233*, 116364. [CrossRef]

38. Henning, M.; Haase, M. Techno-economic analysis of hydrogen enhanced methanol to gasoline process from biomass-derived synthesis gas. *Fuel Process. Technol.* **2021**, *216*, 106776. [CrossRef]

39. Ahmad, M.I.; Zhang, N.; Jobson, M. Integrated design of diesel hydrotreating processes. *Chem. Eng. Res. Des.* **2011**, *89*, 1025–1036. [CrossRef]

40. Gong, L. Molecular Characterisation and Modelling of Hydroprocesses. Ph.D. Thesis, University of Manchester, Manchester, UK, 2017.

41. Gruia, A. Hydrotreating. In *Handbook of Petroleum Processing*; Jones, D., Pujadó, P., Eds.; Springer: Dordrecht, The Netherlands, 2006; pp. 321–354.

42. Benzene, 1,2,4,5-tetramethyl-. Available online: https://webbook.nist.gov/cgi/cbook.cgi?ID=95-93-2 (accessed on 20 November 2020).

43. Benzene, 1,2,3,5-tetramethyl-. Available online: https://webbook.nist.gov/cgi/cbook.cgi?ID=527-53-7 (accessed on 16 February 2021).

44. Benzene, 1,2,3,4-tetramethyl-. Available online: https://webbook.nist.gov/cgi/cbook.cgi?Name=1,2,3,4-tetramethylbenzene (accessed on 16 February 2021).

45. Hidalgo-Vivas, A.; Joensen, F. Process and Catalyst for Upgrading Gasoline. Patent WO2013178375A1, 30 March 2013.

46. Harandi, M. Integrated Process for Converting Methanol to Gasoline and Distillates. Patent US5177279A, 1 October 1991.

47. Bridgwater, A. International construction cost location factors. *Chem. Eng.* **1979**, *86*, 119–121.

48. Towler, G.; Sinnott, R. Capital Cost Estimating. In *Chemical Engineering Design*, 2nd ed.; Elsevier: Amsterdam, The Netherlands, 2012; pp. 307–354.

49. Anonymous. *Technical Information*, Unpublished Confidential Document. 2020.

50. Vogelaar, B. Deactivation of Hydroprocessing Catalysts: New Insights in Catalyst Structure, Activity and Stability. Ph.D. Thesis, Delft University of Technology, Delft, The Netherlands, 2005.

51. Hsu, C.; Robinson, P. Cracking. In *Petroleum Science and Technology*; Hsu, C., Robinson, P., Eds.; Springer, Cham: Amsterdam, The Netherlands, 2019; pp. 211–244.

52. Towler, G.; Sinnott, R. Estimating Revenues and Production Costs. In *Chemical Engineering Design*, 2nd ed.; Elsevier: Amsterdam, The Netherlands, 2012; pp. 355–387.

53. Towler, G.; Sinnott, R. Economic Evaluation of Projects. In *Chemical Engineering Design*, 2nd ed.; Elsevier: Amsterdam, The Netherlands, 2012; pp. 389–429.

54. Drawdowns of Large Corporate Loans High in March 2020. Available online: https://www.suomenpankki.fi/en/Statistics/mfi-balance-sheet/older-news/2020/drawdowns-of-large-corporate-loans-high-in-march-2020 (accessed on 26 January 2021).

55. Petroleum Refining and Related Industries: Average Industry Financial Ratios for U.S. Listed Companies. Available online: https://www.readyratios.com/sec/industry/29 (accessed on 26 January 2021).

56. Nieminen, H.; Laari, A.; Koiranen, T. CO_2 Hydrogenation to Methanol by a Liquid-Phase. *Processes* **2019**, *7*, 405. [CrossRef]

57. Nickel Catalyst with Al2O3 as Carrier for Methanation. Available online: https://www.alibaba.com/product-detail/Nickel-catalyst-with-al2O3-as-carrier_1441840382.html?spm=a2700.galleryofferlist.normal_offer.d_title.1393364edPMXF5 (accessed on 4 June 2021).

58. ZSM-5 Zeolite for Methanol to Gasoline. Available online: https://www.alibaba.com/product-detail/ZSM-5-zeolite-for-methanol-to_62161018217.html?spm=a2700.galleryofferlist.normal_offer.d_title.1393364edPMXF5 (accessed on 4 June 2021).

59. Environmental Markets. Available online: https://www.stx.online/department/all (accessed on 3 December 2020).

60. Hannula, I. Co-production of synthetic fuels and district heat from biomass residues, carbon dioxide and electricity: Performance and cost analysis. *Biomass Bioenergy* **2015**, *74*, 26–46. [CrossRef]

61. Phillips, S.D.; Tarud, J.K.; Biddy, M.J.; Dutta, A. Gasoline from Woody Biomass via Thermochemical Gasification, Methanol Synthesis, and Methanol-to-Gasoline Technologies: A Technoeconomic Analysis. *Ind. Eng. Chem. Res.* **2011**, *50*, 11734–11745. [CrossRef]

62. Rivera-Tinoco, R.; Farran, M.; Bouallou, C.; Auprêtre, F.; Valentin, S.; Millet, P.; Ngameni, J. Investigation of power-to-methanol processes coupling electrolytic hydrogen production and catalytic CO_2 reduction. *Int. J. Hydrogen Energy* **2016**, *41*, 4546–4559. [CrossRef]

63. Directive 2009/30/EC of the European Parliament and of the Council of 23 April 2009. Available online: https://eur-lex.europa.eu/legal-content/EN/TXT/?uri=celex%3A32009L0030 (accessed on 25 September 2020).

64. Jones, D. Quality control of products in petroleum refining. In *Handbook of Petroleum Processing*; Jones, D., Pujadó, P., Eds.; Springer: Dordrecht, The Netherlands, 2006; pp. 705–737.

65. World Jet Fuel Specifications with Avgas Supplement. Available online: http://large.stanford.edu/courses/2017/ph240/chhoa1/docs/exxon-2008.pdf (accessed on 25 September 2020).

66. Material Safety Data Sheet. Available online: https://ch-msds.shell.com/MSDS/000000004706_US_EN.pdf (accessed on 25 September 2020).

67. Zhang, C.; Jun, K.-W.; Gao, R.; Kwak, G.; Park, H.-G. Carbon dioxide utilization in a gas-to-methanol process combined with CO_2/Steam-mixed reforming: Techno-economic analysis. *Fuel* **2017**, *190*, 303–311. [CrossRef]

68. Xiang, Y.; Zhou, J.; Lin, B.; Xue, X.; Tian, X.; Luo, Z. Exergetic evaluation of renewable light olefins production from biomass via synthetic methanol. *Appl. Energy* **2015**, *157*, 499–507. [CrossRef]

69. Anicic, B.; Trop, P.; Goricanec, D. Comparison between two methods of methanol production from carbon dioxide. *Energy* **2014**, *77*, 279–289. [CrossRef]

70. Atsonios, K.; Panopoulos, K.D.; Kakaras, E. Investigation of technical and economic aspects for methanol production through CO_2 hydrogenation. *Int. J. Hydrogen Energy* **2016**, *41*, 2202–2214. [CrossRef]

71. Tremel, A.; Wasserscheid, P.; Baldauf, M.; Hammer, T. Techno-economic analysis for the synthesis of liquid and gaseous fuels based on hydrogen production via electrolysis. *Int. J. Hydrogen Energy* **2015**, *40*, 11457–11464. [CrossRef]

72. Projects Eligible for Aid and Maximum Amount of Aid. Available online: https://tem.fi/en/projects-eligible-for-aid (accessed on 7 December 2020).

73. Questions and Answers: A Hydrogen Strategy for a Climate Neutral Europe. Available online: https://ec.europa.eu/commission/presscorner/detail/en/QANDA_20_1257 (accessed on 27 November 2020).

74. Current Posted Prices. Available online: https://www.methanex.com/our-business/pricing (accessed on 15 March 2021).

75. Biopolttoaineiden Jakeluvelvoite. Available online: https://www.vero.fi/syventavat-vero-ohjeet/ohje-hakusivu/56210/biopolttoaineiden-jakeluvelvoite2 (accessed on 15 March 2021). (In Finnish).

76. Fuels—Higher and Lower Calorific Values. Available online: https://www.engineeringtoolbox.com/fuels-higher-calorific-values-d_169.html (accessed on 15 March 2021).

77. Directive (EU) 2018/2001 of the European Parliament and of the Council of 11 December 2018. Available online: https://eur-lex.europa.eu/eli/dir/2018/2001/oj (accessed on 16 October 2020).

78. Sipilä, E.; Kiuru, H.; Jokinen, J.; Saarela, J.; Tamminen, S.; Laukkanen, M.; Palonen, P.; Nylund, N.-O.; Sipilä, K. *Cost Effective Pathways of Biofuels Until 2030*; Prime Minister's Office: Helsinki, Finland, 2018. (In Finnish)

79. German Biofuel Ticket Market to Get a Boost. Available online: https://www.argusmedia.com/en/news/1734517-german-biofuel-ticket-market-to-get-a-boost (accessed on 16 March 2021).

80. Uusiutuvien Polttoaineiden Liikennekäyttöä Edistävät Lakiluonnokset Lausunnolle. Available online: https://valtioneuvosto.fi/en/-//1410877/uusiutuvien-polttoaineiden-liikennekayttoa-edistavat-lakiluonnokset-lausunnolle (accessed on 26 January 2021). (In Finnish).
81. What Role Is There for Electrofuel Technologies in European Transport's Low Carbon Future? Available online: https://www.transportenvironment.org/sites/te/files/publications/2017_11_Cerulogy_study_What_role_electrofuels_final_0.pdf (accessed on 10 June 2021).